Journal of the European Ceramic Society **19** (1999) 1071–1075

PII: S0955-2219(98)00376-8
0955-2219/99/$ - see front matter

Synthesis and Dielectric Properties of $Ba_{1-x}R_{2x/3}Nb_2O_6$ (R: Rare Earth) with Tetragonal Tungsten Bronze Structure

Naoki Wakiya, Jui-Kai Wang, Atsushi Saiki, Kazuo Shinozaki and Nobuyasu Mizutani*

Department of Inorganic Materials Faculty of Engineering, Tokyo Institute of Technology, 2-12-1, O-okayama, Meguro-ku, Tokyo 152-8552, Japan

Abstract

A series of new compounds, $Ba_{1-x}R_{2x/3}Nb_2O_6$ (R=Nd, Eu, Gd, Tb, Dy, Ho and Er) with tetragonal tungsten bronze (TTB) structure were synthesized. For Ba–R–Nb–O system, single phase TTB was obtained when X = 0·25. To understand the formation condition of these TTB type compounds, two tolerance factors for TTB, t_{A1} and t_{A2}, were proposed against the coordination polyhedra around A1 and A2 site cations, respectively. One of the factors was at least a requisition to stabilize crystal structure for all TTB type compounds. $Ba_{1-x}R_{2x/3}Nb_2O_6$ showed ferroelectric characteristics and the Curie temperature, T_c, increased as the decrease of the ionic radius of rare earth cations. These new compounds have potential to be candidates to apply ferroelectric random access memory (FRAM). © *1999 Elsevier Science Limited. All rights reserved*

Keywords: tetragonal tungsten bronze, C. ferroelectric properties.

1 Introduction

Lately, there has been considerable interest in ferroelectric random access memories (FRAM) since this type of memory does not require a back-up battery to maintain information. FRAMs can be categorized into two types; one is pass-gate arrays type (2T2C type[1] and 1T1C type[2]) and the other is metal-ferroelectric-semiconductor field-effect transistors (MFSFET) type.[3] In the pass-gate arrays type, the information must be read by switching (destructive read-out), therefore, large remanent polarization Pr is required for ferroelectric materials ($P_r > 10\ \mu C\ cm^{-2}$). On the contrary, the MFSFET type has a non-destructive read operation since the +Pr or −Pr polarization of the gate modifies the magnitude of the source-to-drain current, therefore, large Pr is not necessary and smaller Pr ($Pr > 0{\cdot}1\ \mu C\ cm^{-2}$) is enough to operate MFSFET. MFSFET type FRAM is superior to the pass-gate array type since non-destructive read-out is possible and MFSFET type obeys the scaling rule.[4]

For FRAM application, ferroelectric materials should satisfy at least the following 6 conditions: (1) ferroelectricity ($Pr > 0{\cdot}1\ \mu C\ cm^{-2}$ mentioned above), (2) low dielectric constant to improve S/N ratio, (3) low coercive field to lower the drive voltage, (4) high resistivity to prevent leakage, (5) compatibility to silicon technology and (6) high fatigue endurance. So far, $Pb(Zr,Ti)O_3$(PZT) and $SrBi_2Ta_2O_9$ (Y1)[5] are regarded as the most promising materials. In addition to PZT and Y1, some researchers are interested in $YMnO_3$[6] and $Sr_2Nb_2O_7$.[7] Figure 1 shows a 'performance map' for each ferroelectric material. This map illustrates the relative performance from the point of the above 6 conditions. The map shows that PZT is not necessarily good ferroelectric material since it has high dielectric constant and high coercive field as well as low resistivity. Moreover, Pb is detrimental for silicon technology and environment (pollution problem). The map indicates that $Sr_2Nb_2O_7$ is a most promising material, however, it has started to attract attention just last year (1998). This fact suggests that there is a potential to discover new ferroelectric materials which satisfy the above 6 conditions.

In this work, attention was paid to compounds with tetragonal tungsten bronze (TTB) structure.

*To whom correspondence should be addressed. Fax: +81-3-5734-2519; e-mail: nmizutan@ceram.titech.ac.jp

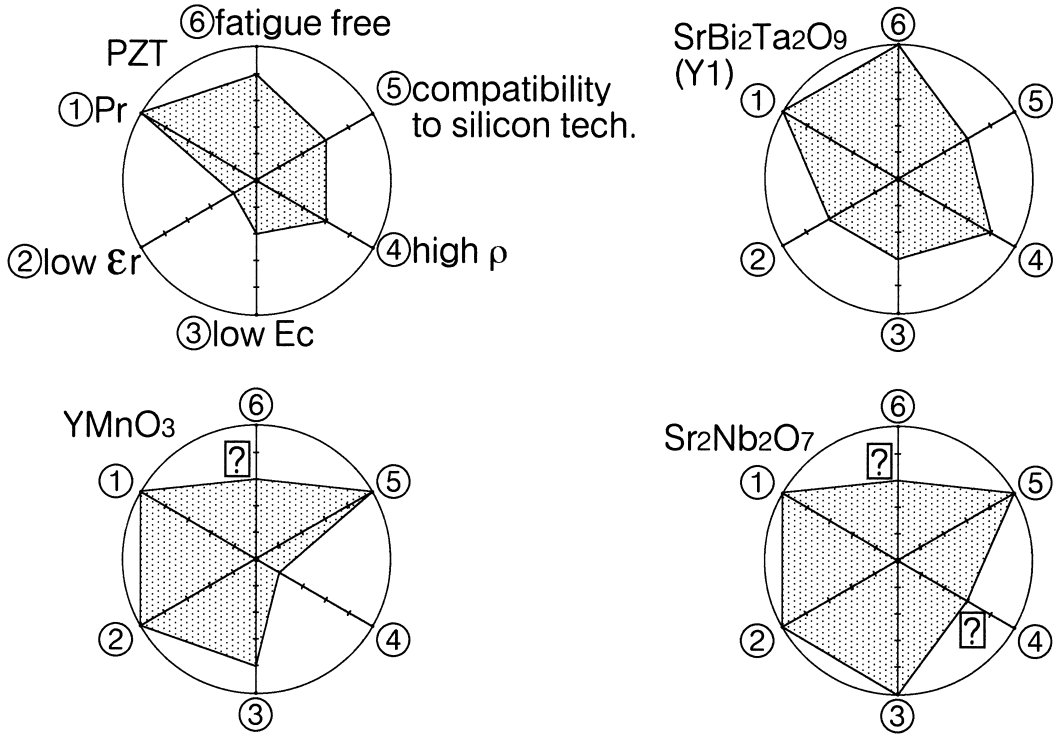

Fig. 1. 'Performance map' for MFS FET type FRAM application for $Pb(Zr,Ti)O_3$ (PZT), $SrBi_2Ta_2O_9$ (Y1), $YMnO_3$ and $Sr_2Nb_2O_7$.

The merit of TTB is that it has high anisotropy of crystal structure ($a = 1{\cdot}2$ nm and $c = 0{\cdot}4$ nm), therefore on the deposition of thin film, c-axis orientation is easily obtained[8,9] which direction is expected to coincides with the direction of polarization. Figure 2 shows a 'performance map' for $Sr_{2{\cdot}3}Ba_{2{\cdot}7}Nb_{10}O_{30}$. (SBN46) which is representative of TTB compounds. This map shows that SBN46 is not necessarily fit for FRAM, however, if the dielectric constant can be decreased and resistivity can be increased, TTB has the potential to be a candidate for FRAM.

The target of this work is to search for new compounds with TTB structure by the substitution of Ba^{2+} in $BaNb_2O_6$ with R^{3+} (R: rare earth)

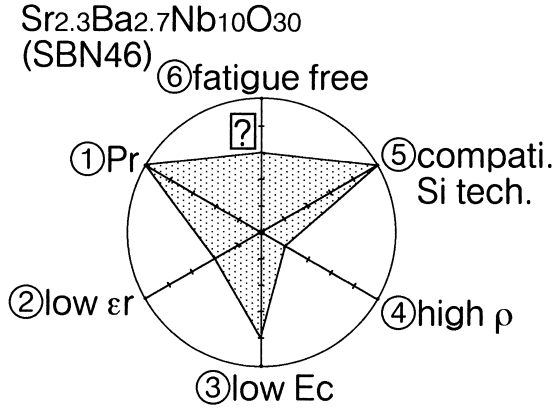

Fig. 2. 'Performance map' for MFS FET type FRAM application for $Sr_{2{\cdot}3}Ba_{2{\cdot}7}Nb_{10}O_{30}$ (SBN46).

cations, and consider formation conditions of TTB from the point of crystal chemistry. In addition, potential in FRAM application was also considered. TTB type compounds in Ba–R–Nb–O system have only been reported for R = Y, Sm and La[10], however, substitution by other elements is not reported. Moreover in the literature,[10] the formation condition of TTB and its potential for use in FRAM are not considered.

2 Experimental

The specimens were prepared by a conventional solid state reaction from starting materials of reagent grade $BaCO_3$, R_2O_3 (R: La-Yb) and Nb_2O_5. These starting materials were weighted according to the following composition: $Ba_{1-x}R_{2x/3}Nb_2O_6$ where $X = 0{\cdot}1 - 0{\cdot}6$ for Y, and $X = 0{\cdot}25$ for other rare earth elements. The powders were mixed by ball-milling in ethanol with zirconia balls for 20 h. The resultant slurries were then dried using a rotary evaporator. The powder mixtures were pressed into pellets and calcined at 900 °C for 2 h in air. Then the pellets were ground and pressed into pellets. The pellets were put in the platinum crucible and sintered at 1300 °C for 4 h in air. After polishing, platinum paste was painted on the surface of the pellet and dielectric properties (4192A, Hewlet–Packard) and P-E hysteresis curves (RT-66A, Radiant Technology) were measured.

3 Results and Discussion

3.1 Formation of new compounds and their crystal chemistry

For $Ba_{1-x}Y_{2x/3}Nb_2O_6$, composition, single phase TTB was formed when $X = 0{\cdot}25$ which agrees with the literature.[10] TTB compounds were synthesized for R=La, Nd, Sm, Gd, Tb, Dy, Ho and Er in $Ba_{0{\cdot}75}R_{0{\cdot}1667}Nb_2O_6$ i.e. TTB for R=Nd, Gd, Tb, Dy, Ho and Er are new compounds. Single phase TTB were obtained except for R=Ho. The reason why single phase TTB was not obtained for R=Ho is ascribed to the mixing problem that this sample only, was mixed without ball milling.

For perovskite structure, the tolerance factor (t) is a parameter to estimate the stability of the crystal structure. For Bismuth Layer-Structured Ferroelectrics (BLSF), tolerance factor t also plays an important role to prescribe the stability of the crystal structure.[11] In this work, the tolerance factor for TTB structure is introduced. General formula of TTB is $(A1)_2(A2)_4(B1)_2(B2)_8(O1)_8(O2)_8(O3)_4(O4)_2(O5)_4(O6)_4$. According to this general formula, the compounds synthesized in this work is denoted as $Ba_{3{\cdot}75}R_{0{\cdot}833}Nb_{10}O_{30}$). Figure 3 shows projection of TTB structure along [001]. As shown in this figure, TTB has two kinds of A sites. A1 cations are 12-fold coordination and the coordination polyhedra is identical to that in perovskite structure, therefore tolerance factor for A1 site cation (t_{A1}) can be given by the following equation:

$$t_{A1} = \frac{(r_{A1} + r_o)}{\sqrt{2}(r_B + r_o)} \qquad (1)$$

On the other hand, A2 cations occupy pentagonal site and their coordination number is 15. The coordination polyhedra was shown in Fig. 4. In the coordination polyhedra, it is reported that the interatomic distances between A2 and four O(1), two O(3) and O(4) is shorter than other distances.[12] Therefore from the geometrical consideration, tolerance factor for A2 site cation (t_{A2}) can be expressed in the following equation:

$$t_{A2} = \frac{(r_{A2} + r_o)}{\sqrt{23 - 12\sqrt{3}}(r_B + r_o)} \qquad (2)$$

For $Ba_{3{\cdot}75}R_{0{\cdot}833}Nb_{10}O_{30}$, the result of Rietveld analysis using powder diffraction data and site potential calculation revealed that R^{3+} cation occupies A1 site and Ba^{2+} cation occupies A2 site. The detail of this structure refinement will be written in the literature.[13] Figure 5 shows the relationship between t_{A1} and t_{A2}. In this figure, open circles denote TTB compounds reported in the literature[14] and closed circles denote compounds synthesized in this work. This figure indicates that the compound with R=Er has the smallest t_{A1} ($=0{\cdot}892$) in the $Ba_{3{\cdot}75}R_{0{\cdot}833}Nb_{10}O_{30}$ series, and also indicates that the t_{A1} value (0·892) is the smallest for all reported TTB compounds. Therefore it is expected

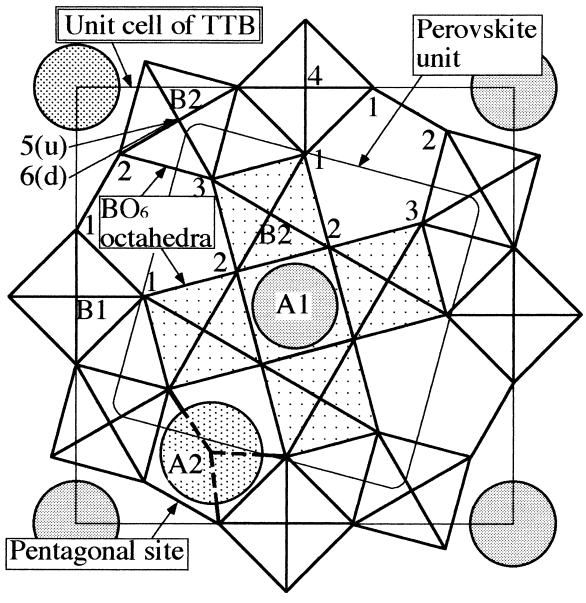

Fig. 3. Projection of TTB structure along [001].

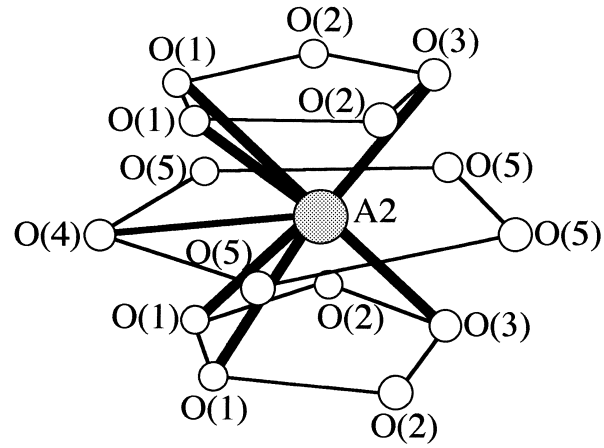

Fig. 4. Coordination polyhedra around A2 cation in TTB.

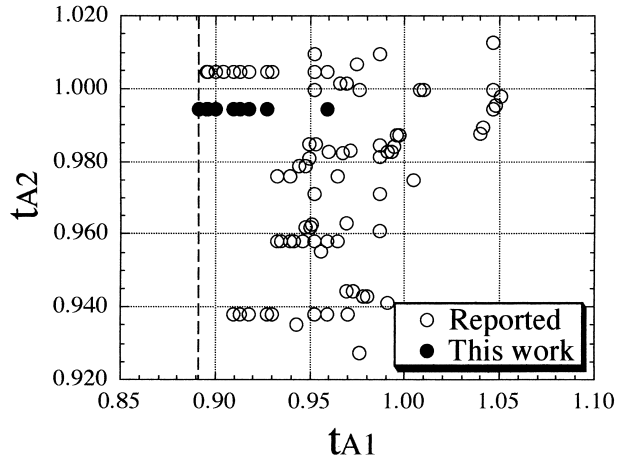

Fig. 5. Relationship between t_{A1} and t_{A2}.

that this value is a lower limit and a requisition for the stabilization of TTB. In this work, Ba^{2+} was fixed as the A2 cation, therefore such a requisition cannot he found for t_{A2}.

3.2 Characteristics of new compounds

The relative densities of the sintered pellets are over 90% of their theoretical ones. Figure 6 shows the temperature dependence of dielectric constant for $Ba_{3.75}R_{0.833}Nb_{10}O_{30}$. This figure indicates that dielectric constants at room temperature for R=Ho, Er and Y lie between 180 and 260, these values are much smaller than that for SBN46[14] (500). Figure 7 shows the change of Curie temperature (T_c) with ionic radii of rare earth cations for $Ba_{3.75}R_{0.833}Nb_{10}O_{30}$. This figure shows that TTB compound with a small ionic radii of rare earth cation have high T_c. Figure 8 shows P-E hysteresis curves for $Ba_{3.75}R_{0.833}Nb_{10}O_{30}$ for R=Er, Ho, Y and Gd. This figure indicates that Pr

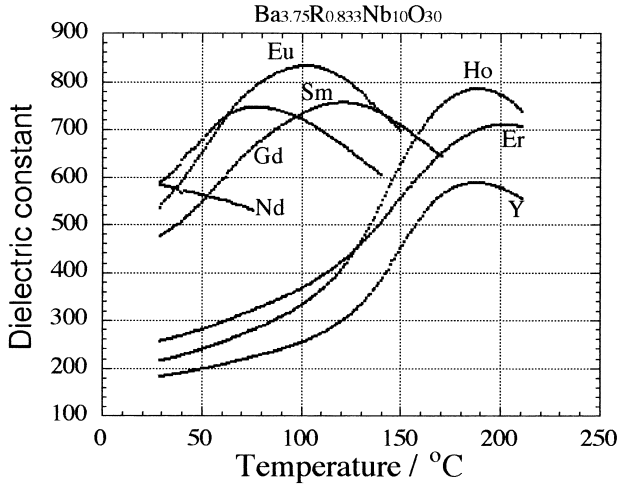

Fig. 6. Temperature dependence of dielectric constant for $Ba_{3.75}R_{0.833}Nb_{10}O_{30}$.

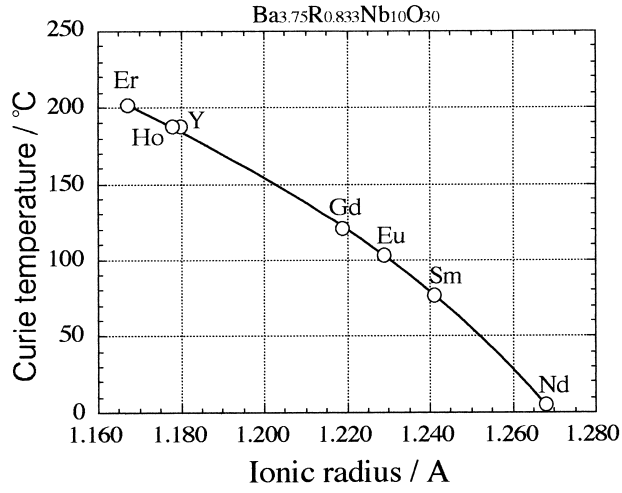

Fig. 7. Change of T_c with ionic radii of rare earth cations.

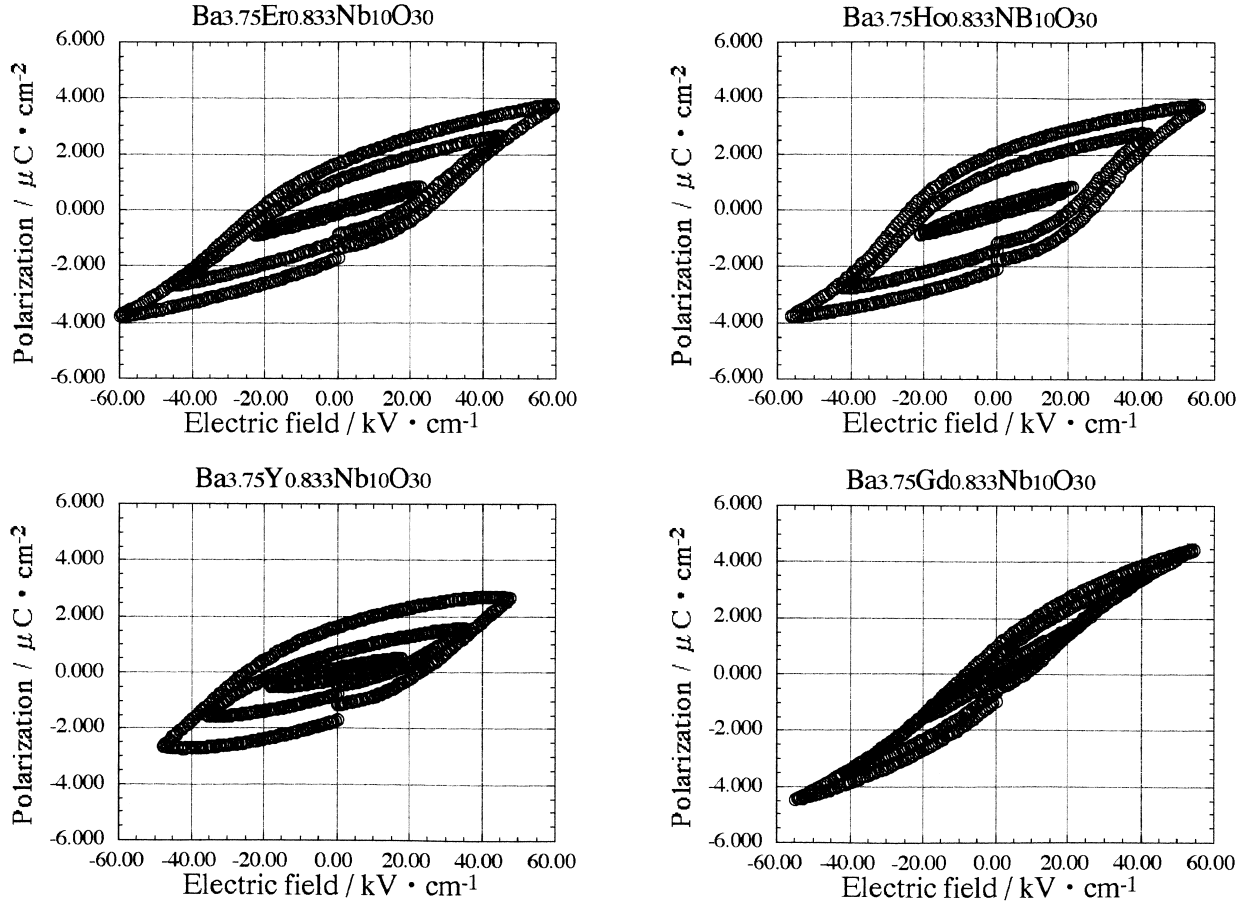

Fig. 8. P-E hysteresis for $Ba_{3.75}R_{0.833}Nb_{10}O_{30}$ (R=Er, Ho, Y and Gd).

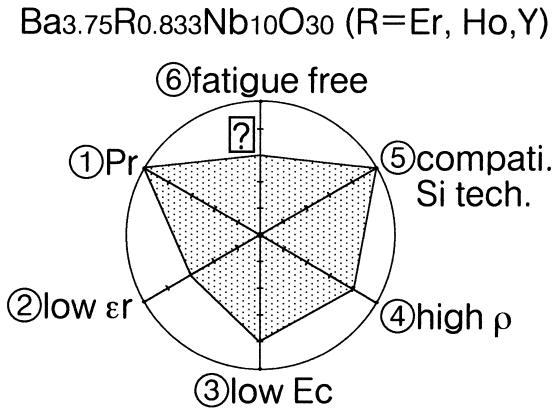

Fig. 9. 'Performance map' for MFS FET type FRAM application for $Ba_{3.75}R_{0.833}Nb_{10}O_{30}$ (R=Er, Ho and Y).

for these compounds are between 1 and 2 $\mu C\,cm^{-2}$, and Ec are between 10 and 30 $kV\,cm^{-1}$. Moreover, the resistivity of these compounds is 10^{-8} ohm·m order. The results shown in Figs 7 and 8 indicate that the TTB compounds are sufficient for FRAM application. Therefore the 'performance map' for $Ba_{3.75}R_{0.833}Nb_{10}O_{30}$ (R=Er, Ho and Y) can be drawn as Fig. 9. Comparing Fig. 9 with Fig. 2, it can be mentioned that the performances of the new TTB compounds investigated in this work are superior to reported TTB compounds (SBN46) and have potential for use in FRAM.

4 Conclusions

Tetragonal tungsten bronze compound with general formula, $Ba_{3.75}R_{0.833}Nb_{10}O_{30}$ (R=La, Nd, Sm, Eu, Gd, Tb, Dy, Ho and Y), were synthesized. These compounds, except R=La, Sm and Y were new compounds. For Ba–R–Nb–O system, single phase TTB was obtained when $X = 0{\cdot}25$. To understand the formation condition of these TTB type compounds, two tolerance factors for TTB, t_{A1} and t_{A2}, were proposed against polyhedra around A1 and A2 site cations, respectively. It was clarified that t_{A1} is a requisition to stabilize crystal structure for all TTB type compounds. $Ba_{1-x}R_{2x/3}Nb_2O_6$ showed ferroelectric characteristics and the Curie temperature, T_C, increased as the decrease of the ionic radius of rare earth cations. These new compounds have potential to be candidates to apply ferroelectric random access memory (FRAM).

References

1. Evans, J. T. and Womack, R. *IEEE J. Solid State Circuits*, 1988, **23**, 1171.
2. Eaton, S. S., Butler, D. B., Parris, M., Wilson, D. and MeNeillie, H., *Proc. IEEE Int. Solid-State Circuits Conference*, 1988.
3. Moll, J. L. and Tarui, Y., *IEEE Trans. Electron Devices*, 1963, **10**, 338.
4. Nakamura, T., Nakano, Y., Kamisawa, A. and Takasu, H., *IEEE Int. Solid-State Circuit Conf., Digest of Technical Papers, WP 4.3*, 1995, p. 68.
5. Paz de Araujo, C. A., Cuchiaro, J. D., McMillan, L. D., Scott, M. C. and Scott, J. F., *Nature*, 1995, **374**, 627.
6. Fujimura, N., Ishida, T., Yoshimura, T. and Ito, T., *Appl. Phys. Lett.*, 1996, **69**, 1011.
7. Fujimori, T., Izumi, N., Nakamura, T., Kamizama, A. and Shigematsu, Y., *Jpn, J. Appl. Phys.*, **37**, (in press).
8. Thony, S. S., Youden, K. E., Harris Jr, J. S. and Hesselink, L., *Appl. Phys. Lett.*, 1994, **65**, 2018.
9. Lin, W. J., Tseng, T. Y., Lin, S. P., Tu, S. L., Yang, S. J., Harn, J. J., Liu, K. S. and Lin, I. N., *Jpn. J. Appl. Phys.*, 1995, **34**, L625.
10. Masuno, K., *J. Phys. Soc. Jpn*, 1964, **19**, 323.
11. Subbarao, E. C., *J. Am. Ceram. Soc.*, 1962, **45**, 166.
12. Sciau, P., Lu, Z., Calvarin, G., Roisnel, T. and Ravez, J., *Mat. Res. Bull.*, 1993, **28**, 1233.
13. Wakiya, N., Wang, J. K., Saiki, A., Shinozaki, K. and Mizutani, N., *J. Korean Ceramic Soc.* (in press).
14. *Landolt-Bornstein, New Series III/16a*, 170, Springer-Verlag, Berlin, Heidelberg, New York, 1981.